ANNALS OF FACULTY ENGINEERING HUNEDOARA
– INTERNATIONAL JOURNAL OF ENGINEERING
Tome X (Year 2012) – FASCICULE 3 (ISSN 1584 – 2673)

[1.] Diana Alina BISTRIAN

L^2 – PROJECTION METHOD FOR HYDRODYNAMIC EIGENVALUE PROBLEMS

[1.] "POLITEHNICA" UNIVERSITY OF TIMISOARA, FACULTY OF ENGINEERING OF HUNEDOARA, DEPARTMENT OF ELECTRICAL ENGINEERING AND INDUSTRIAL INFORMATICS, ROMANIA

ABSTRACT: *This paper reports a numerical method to compute eigenvalue problems arising in hydrodynamic instability problems. An L^2 – projection type algorithm is developed assessing both analytical methodology and implementation using symbolic and numerical conversions and applied to a particular case of the trailing vortices developed by delta wings aircrafts. The results of the swirling system instability are pointed out, together with the advantages of using the algorithm in flow control problems.*
KEYWORDS: *hydrodynamic instability, projection method, spectral algorithms*

INTRODUCTION

Swirling flows behavior has long been an intensive subject of research. The amount of computational resources required to accurately simulate swirling systems is huge, so a complementary stability analysis is a critical requirement to predict the flow dynamics. Pozrikidis [10] offer an introductory course in fluid mechanics, covering the traditional topics in a way that unifies theory, computation, computer programming and numerical simulation. Resiga et al. [12] carried out an experimental and theoretical investigation of the processing helical vortex developed at the outlet of a Francis turbine runner, in order to elucidate the causes of a sudden drop in the draft tube pressure recovery coefficient at a discharge near the best efficiency operating point.

The objective of this paper is to present new instruments that can provide relevant conclusions on the stability of swirling fluid systems assessing both an analytical methodology and numerical methods for a spatial stability investigation of the bending modes [1].

The mathematical model governing the linear spatial stability of the swirling fluid system, corresponding to the values of tangential wavenumber $m=\pm 1$, in operator form is

$$\Lambda_1(k,F,G,H,P)=\frac{d}{dr}(rG)+k\,r\,F+G+m\,H\,, \tag{1}$$

$$\Lambda_2(k,F,G,H,P)=kUG-\omega G+\frac{mWG}{r}+\frac{2WH}{r}-\frac{d}{dr}P\,, \tag{2}$$

$$\Lambda_3(k,F,G,H,P)=kHU-H\omega+\frac{m}{r}[HW+P]+\frac{WG}{r}+G\frac{d}{dr}W\,, \tag{3}$$

$$\Lambda_4(k,F,G,H,P)=kFU-F\omega+\frac{mFW}{r}+G\frac{d}{dr}U+kP\,, \tag{4}$$

where $\{F,G,H,P\}(r)$ represent the complex amplitudes of the perturbations, k is the complex axial wavenumber, m is the integer tangential wavenumber, ω represents the temporal frequency, U and W represent the axial and the tangential velocity, respectively, both depending only on the radial coordinate r.

For a given real ω, the system (1)-(4) is equivalent to the complex eigenvalue problem

$$\Lambda_1=\Lambda_2=\Lambda_3=\Lambda_4=0 \tag{5}$$

on the domain $(0,r_{wall})$ together with the boundary conditions in axis origin

$$H\pm G=0,\quad F=P=0 \tag{6}$$

and the wall boundary conditions

$$\frac{2W_{rwall}H}{r_{wall}}-P'=0,\quad G=0, \tag{7a}$$

$$r_{wall}H(kU_{rwall}-\omega)\pm HW_{rwall}\pm P=0=0, \tag{7b}$$

$$r_{wall}F(kU_{rwall}-\omega)\pm FW_{rwall}+kr_{wall}P=0\,. \tag{7c}$$

where U_{rwall} and W_{rwall} are the axial and the tangential velocity respectively, calculated at domain limit r_{wall} and prime denotes the differentiation with respect to the radius.

The hydrodynamic stability model developed in the forthcoming sections of this paper involves spectral differentiation operators derived by means of shifted orthogonal expansions of the perturbation field. The hydrodynamic model presented in Section 2 is developed using an L^2 – projection method with operator scheme. The sophisticated boundary conditions motivated the use of this method, suitable for non-periodic problems with complicated boundary conditions.

Dongara [6] used the Chebyshev tau method to examine in detail a variety of eigenvalue problems arising in hydrodynamic stability studies, particularly those of Orr-Sommerfeld type. The orthogonality of Chebyshev functions was used by Bourne [4] to rewrite the differential equations as a generalized eigenvalue problem, assembling a very efficient projection based technique.

The classical approaches imply a transformation of the physical domain onto the standard interval for the definition of the Chebyshev polynomials. For the approach presented in this paper, instead of using classical Chebyshev polynomials, we used shifted Chebyshev polynomials, directly defined on the physical domain of the problem, preserving the orthogonality properties detailed in Section 2.1. The numerical algorithm was developed to work automatically for any number of expansion terms, using symbolic and numeric conversions, the implementation technique being detailed in Section 2.2. In Section 3 the algorithm is validated upon the model of a trailing vortex. An error analysis is performed in Section 4 and the algorithm is efficiently improved by a numerical procedure for eliminating the spurious eigenvalues form the hydrodynamic spectra. The main results of the paper are summarized in Section 5.

L^2 – PROJECTION ALGORITHM FOR BENDING MODES – Methodology

Following [4] the eigenvalue problem is transformed into a system of linear equations describing the hydrodynamic context for the cases $m=\pm 1$.

The difference between the classical tau method and the modified version proposed here is given by the selected spaces involved in the approximation process. An appropriate solution is sought in the truncated Chebyshev series form

$$(F,G,H,P)=\sum_{k=1}^{N}(f_k,g_k,h_k,p_k)\cdot T_k^*, \tag{8}$$

with $f_k,g_k,h_k,p_k,k=1..N$ the sets of expansions coefficients to be found. The tau method is an algorithm implying in the first step expanding the residual function as a series of shifted Chebyshev polynomials.

Since the range $[0,r_{wall}]$ is more convenient to use than the standard definition interval of classical Chebyshev polinomials $[-1,1]$ to discretize our hydrodynamic stability problem, where r_{wall} represents the radial distance to the wall of the computational domain, we map the independent variable $r\in[0,r_{wall}]$ to the variable $\xi\in[-1,1]$ by the linear transformation

$$\xi=2rr_{wall}^{-1}-1 \quad\Leftrightarrow\quad r=r_{wall}(\xi+1)2^{-1}. \tag{9}$$

The shifted Chebyshev polynomials of the first kind $T_n^*(r)$ of degree $n-1$ in r on $[0,r_{wall}]$ are given by

$$T_n^*(r)=T_n(\xi)=T_n\left(2rr_{wall}^{-1}-1\right). \tag{10}$$

The shifted Chebyshev class is orthogonal in the Hilbert space $L_w^2(0,r_{wall})$, weighted by $w(r)=\left(1-\left(2rr_{wall}^{-1}-1\right)\right)^{-1/2-1}$. They have the next orthogonality properties

$$\left(T_n^*,T_m^*\right)_w=0\ ,\ n\neq m\ ,\quad n,\ m=1..N\ , \tag{11}$$

$$\left(T_n^*,T_n^*\right)_w=r_{wall}\frac{\pi}{\lambda},\quad \lambda=\begin{cases}2 & if \quad n=1\\ 4 & if \quad n=2..N\end{cases}, \tag{12}$$

with respect to the inner product $(u,v)_w=\int_0^{r_{wall}} wuv\,dr$.

The differential model is reduced to a finite dimensional algebraic system in the expansion coefficients only by imposing the condition that each equation of the system to be orthogonal with respect to the inner product $\left(\Lambda_i,T_j^*\right)_w$, $i=1..4$, $j=0,..,N-2$ in the Hilbert space $L_w^2(0,r_{wall})$. We obtain a set of $4(N-2)$ linear equations. The eight remaining equations are provided by the boundary conditions applied as side constraints.

Introducing the notations

$$I_{ijkld}^{U}=\left(r^k(U^l)^{(d)}T_i^*,T_j^*\right)_w,\quad I_{ijkld}^{W}=\left(r^k(W^l)^{(d)}T_i^*,T_j^*\right)_w \tag{13}$$

with (d) *the derivation order, the first truncated* $4(N-2)$ *equations of the hydrodynamic stability model become*

$$k\sum_{j=1}^{N}\left(f_j I^U_{ij100}\right)+g_i r_{wall}c+g_2\frac{2}{r_{wall}}I^U_{i1100}+\sum_{\substack{j=3\\ j\ odd}}^{N}g_j\frac{2(j-1)}{r_{wall}}\left[\sum_{\substack{r=j-1\\ j\ even}}^{2}2I^U_{ir100}\right]+$$

$$+\sum_{\substack{j=4\\ j\ even}}^{N}g_k\frac{2(j-1)}{r_{wall}}\left[\sum_{\substack{r=j-1\\ j\ odd}}^{2}\left(2I^U_{ir100}\right)+I^U_{i1100}\right]+mh_i r_{wall}c=0, \tag{14}$$

$$k\sum_{j=1}^{N}g_j I^U_{ij010}-\omega g_i r_{wall}c+m\sum_{j=1}^{N}g_j I^W_{ij-110}+2\sum_{j=1}^{N}h_j I^W_{ij-110}-p_2\frac{2}{r_{wall}}A_{i1}-$$

$$-\sum_{\substack{j=3\\ j\ odd}}^{N}p_j\frac{2(j-1)}{r_{wall}}\left[\sum_{\substack{r=j-1\\ j\ even}}^{2}2A_{ir}\right]-\sum_{\substack{j=4\\ j\ even}}^{N}p_j\frac{2(j-1)}{r_{wall}}\left[\sum_{\substack{r=j-1\\ j\ odd}}^{2}\left(2A_{ir}\right)+A_{i1}\right]=0, \tag{15}$$

$$k\sum_{j=1}^{N}h_j I^U_{ij110}-\omega\sum_{j=1}^{N}h_j I^U_{ij100}+m\sum_{j=1}^{N}h_j I^W_{ij010}+\text{-}m\,p_i r_{wall}c+\sum_{j=1}^{N}g_j\left(I^W_{ij010}+I^W_{ij111}\right)=0, \tag{16}$$

$$k\left(\sum_{j=1}^{N}f_j I^U_{ij010}+p_i\,r_{wall}c\right)-\omega f_i\,r_{wall}c+m\sum_{j=1}^{N}f_j I^W_{ij-110}+\sum_{j=1}^{N}g_j I^U_{ij011}=0, \tag{17}$$

for $i=1..N-2$, *where the number c being defined as* $c=\begin{cases}\pi/2, & i=1\\ \pi/4, & i=2..N-2\end{cases}$ *and* $A\in M_{N-2}$ *is square* $(N-2)\times(N-2)$ *matrix, with* $A_{11}=r_{wall}\pi/2$, $A_{mm}=r_{wall}\pi/4$, $m=2..N-2$, $A_{mn}=0$, $m\neq n$. *Similarly, we translate the boundary conditions in linear equations that complete the system.*

For the case $m=\pm1$ *that we investigate here, the boundary conditions provide the seven equations set:*

$$\sum_{1}^{N}(-1)^{k+1}g_k\pm\sum_{1}^{N}(-1)^{k+1}h_k=0, \tag{18}$$

$$\sum_{1}^{N}(-1)^{k+1}f_k=\sum_{1}^{N}(-1)^{k+1}p_k=0, \tag{19}$$

$$\sum_{1}^{N}g_k=0, \tag{20}$$

$$k\sum_{1}^{N}f_k+\frac{1}{r_{wall}}\sum_{1}^{N}h_k=0, \tag{21}$$

$$\frac{-2W_{wall}}{r_{wall}}\sum_{1}^{N}h_k+p_2\frac{2}{r_{wall}}+\sum_{\substack{3\\ k\ odd}}^{N}p_k\frac{2(k-1)}{r_{wall}}\left[\sum_{\substack{r=k-1\\ k\ even}}^{2}2\right]+\sum_{\substack{4\\ k\ even}}^{N}p_k\frac{2(k-1)}{r_{wall}}\left[\sum_{\substack{r=k-1\\ k\ odd}}^{2}2+1\right]=0, \tag{22}$$

$$kU_{wall}\sum_{1}^{N}h_k+\left(\frac{\pm W_{wall}}{r_{wall}}-\omega\right)\sum_{1}^{N}h_k\pm\frac{1}{r_{wall}}\sum_{1}^{N}p_k=0, \tag{23}$$

$$k\left(U_{wall}\sum_{1}^{N}f_k+\sum_{1}^{N}p_k\right)+\left(\frac{\pm W_{wall}}{r_{wall}}-\omega\right)\sum_{1}^{N}f_k=0. \tag{24}$$

For this case, the additional relation in obtained from the second equation of the mathematical model (2), taking the inner product $\left(\Lambda_2,T^*_{N-1}\right)_w$

The eigenvalue problem is written as a system of 4N equations with the matrix formulation $kM_k\bar{s}=M\bar{s}$, $\bar{s}=\left(\bar{f},\bar{g},\bar{h},\bar{p}\right)$, *with* $\bar{*}=\left(*_1,...,*_N\right)$, $*\equiv f,g,h,p$.

The method has the obvious advantage that the highest degree of the Chebyshev polynomials multiplying the residual in the method inner-product is only $N-2$.

IMPLEMENTATION TECHNIQUE USING SYMBOLIC AND NUMERIC CONVERSIONS

The recurrence relation for T^*_n *has the form*

$$T^*_n(r)=2\left(2rr^{-1}_{wall}-1\right)\cdot T^*_{n-1}(r)-T^*_{n-2}(r),\ n=3,4,... \tag{25}$$

in which the initial conditions are $T_1^*(r)=1, T_2^*(r)=\frac{2r}{r_{wall}}-1$. *The use of a recurrence relation significantly increases the elapsed time to generate the shifted Chebyshev polynomials. To improve the performance of the numerical algorithm, we introduce in our code the equivalent polynomial relation*

$$T_n^*(r)=\frac{1}{2}\left[\left(\tilde{r}+\sqrt{\tilde{r}^2-1}\right)^{n-1}+\left(\tilde{r}-\sqrt{\tilde{r}^2-1}\right)^{n-1}\right],\ \tilde{r}=2rr_{wall}^{-1}-1 \qquad (26)$$

to automatically generate the shifted Chebyshev polynomials $\left\{T_n^*(\xi)\right\}_{n\geq 1}$ *on* $[0,r_{wall}]$.

A modified Chebyshev-Gauss grid $\Xi=(\xi_j)_{1\leq j\leq N}$ *in* $[-1,1]$ *was constructed*

$$\xi_{j+1}=cos\left(\pi+\frac{j\pi}{N-1}\right),\ \xi_{j+1}\in[-1,1],\ j=0..N-1, \qquad (27)$$

mapped into the physical range of our problem by the simple linear transformation $r_i=r_{wall}(\xi_i+1)/2, i=1..N$.

The collocation nodes clustered near the boundaries diminishing the negative effects of the Runge phenomenon [5]. Another aspect is that the convergence of the interpolation function on the clustered grid towards unknown solution is extremely fast. The numerical algorithm was developed to work automatically for any number of expansion terms, using the routines of a high level language such Matlab.

Using the sym2string [15] function the symbolic integrands are converted into a Matlab equation strings.

The symbol @(x) is concatenated to the integrands by using the Matlab strcat [16] procedure and the integrals are delivered as Matlab functions by eval [17] function.

The integrals are evaluated on the physical domain $[0, r_{wall}]$ *using quad [18] Matlab function that numerically evaluates the integrals using an recursive adaptive Simpson quadrature.*

We list in Appendix the code sequences for generating the inner products I_{ijkld}^U.

The generalized eigenvalue problem was solved during numerical simulations by an Arnoldi type algorithm implemented in the sptarn [19] Matlab's procedure.

The application returns an acceptably accurate approximation of the spectrum and relevant information on perturbation amplitudes for stable or unstable modes, the maximum amplitude of the most unstable mode and the critical distance where the perturbation is the most amplified.

NUMERICAL RESULTS OF THE INSTABILITY INVESTIGATION

The basic flow under consideration for the validation of the proposed methods is the Batchelor vortex case or the q-vortex [2] that trails on the tip of each delta wing of the airplanes. The properties of the Batchelor vortex were pointed out in [9] using a shooting method. In order to compare our results with the ones from [9] numerical evaluations of the axial wavenumber k of the most amplified perturbed wave, obtained for various values of the spectral parameter N. In Table 1 these values are presented in comparison with the ones from Olendradru et al. [9] and the ones obtained using the collocation POD (Proper Orthogonal Decomposition) method in our previous investigation [3]. The numerical results obtained by collocation are better, however, the projection method allowed us to investigate the hydrodynamic models with sophisticated boundary conditions.

Table 1. Comparative results of the most amplified spatial wave of the Batchelor-vortex: eigenvalue with largest imaginary part $k_{cr}=(k_r,k_i)$.

$m=1$	$m=-1$
Shooting method [9]	
$k_{cr}=(0.6,0)$	$k_{cr}=(0.454,-1.276)$
POD collocation [3]	
$k_{cr}=(0.5611,0)$	$k_{cr}=(0.76146,-0.33722)$
L^2- *Projection method*	
$k_{cr}=(0.49,0)$	$k_{cr}=(0.57,-1.358)$

The figure 1 illustrate the behavior of the perturbation amplitudes for bending modes, computed with the critical axial wavenumbers listed in Table 1, in comparison with the results obtained in [9].

Following Tadmor [13], when differencing analytic functions using Chebyshev pseudospectral methods, the error committed is expected to decay to zero at an exponential rate. The convergence behavior of the algorithm with respect to the number of expansion terms is shown in Table 2 in comparison with ones obtained using the radial boundary adapted technique in our previous investigations [3].

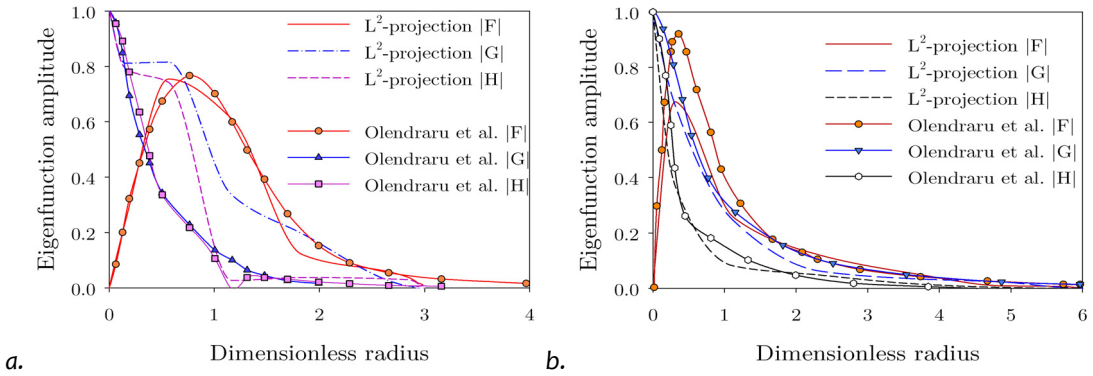

Figure 1. Absolute values of eigenfunction amplitudes computed at:

a) $m=1,\ a=0,\ q=0.7,\ \omega=0.0425,\ k_{cr}=(0.49,0)$ *using* $N=7$ *expansion terms.*

b) $m=-1,\ a=-1.268,\ q=0.6,\ \omega=-0.78,\ k_{cr}=(0.57,-1.358)$ *using* $N=8$ *expansion terms.*

Clearly the numerical computation costs were less expansive in the projection method approach since the number of terms in the approximations was significantly reduced. In fact, in comparison with the boundary adapted collocation method this number was more than twenty times reduced. In consequence, with a reduced by far computational time, we can obtain accurate results in an acceptable agreement with existing ones.

Table 2. Comparison of the convergence behavior of the algorithm assessing POD collocation method and L^2 - projection method

N	Axial wavenumber k_{cr}
POD collocation [3]	
50	0.683678763452345 - 0.314534285467895*i*
110	0.761672356543287 - 0.324782356487634*i*
130	0.763782346791254 - 0.328723914726345*i*
165	0.761466589641356 - 0.337228396511943*i*
L^2 - Projection	
5	0.325249174525684 – 1.084625097561478*i*
6	0.491576258945131 – 1.184214359658741*i*
7	0.551854623988265 – 1.371519652384657*i*
8	0.570546235874152 – 1.358152468512479*i*

ERROR ANALYSIS AND ELIMINATING THE SPURIOUS EIGENVALUES

Although the projection method is a very efficient technique, the inclusion of the boundary conditions as equations in the system of the generalized eigenvalue problem have been observed to be one cause of spurious eigenvalues.

The spurious eigenvalues, which are not always easy to identify, may lead one to a false conclusion regarding the stability of the fluid system, thus the elimination of them is of great importance. These are values returned by the algorithm which do not satisfy the eigenvalue problem. The spurious eigenvalues problems have been the attention of much study recently. Gardner et al. [7] and McFadden et al. [8] describe the tau methods to avoid spurious eigenvalues and in Dongara [6] the occurrence of the spurious eigenvalues is assessed in application to the Benard convection problem.

We implement in our numerical procedure a code sequence that identifies if an eigenvalue of the spectra is spurious or not. First the algorithm provides the entire spectra, then calculates the residual vector of the eigenvalue problem

$$E^k = k\cdot \mathrm{T}\cdot \bar{\mathrm{v}} - \Psi\cdot \bar{\mathrm{v}},\quad \bar{\mathrm{v}} = \left(\bar{f},\bar{g},\bar{h},\bar{p}\right)^T \tag{28}$$

with

$$\left(\bar{f},\bar{g},\bar{h},\bar{p}\right)^T = \left(\{f_k\}_{k=1}^N,\{g_k\}_{k=1}^N,\{h_k\}_{k=1}^N,\{p_k\}_{k=1}^N\right)^T \tag{29}$$

for each eigenvalue of the spectra.

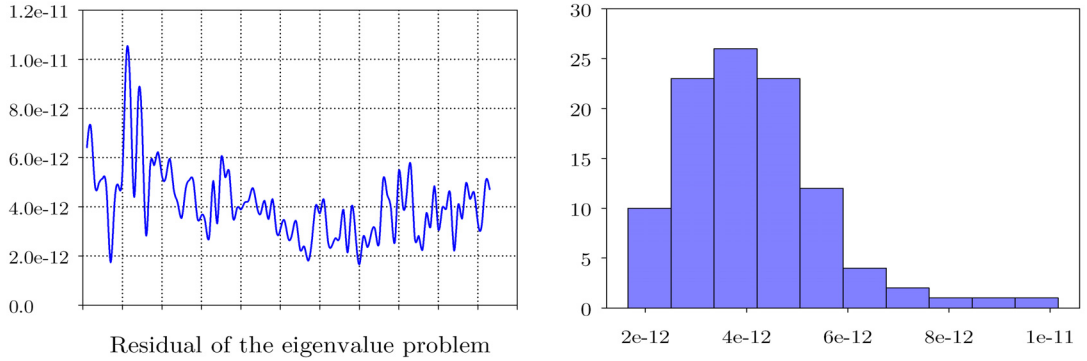

Figure 2. Residual of the eigenvalue problem and corresponding histogram

A true value of k must satisfy the eigenvalue problem. We evaluate the L^2 norm of the vector with respect to a given tolerance ε . If the condition

$$\left(\sum abs\left(E^k\right)^2\right)^{1/2} > \varepsilon \tag{30}$$

holds, the eigenvalue k is declared spurious and discarded form the spectra. Figure 2 presents the residual of the eigenvalue problem, solved using the QZ algorithm implemented in the high level computing platform Matlab and the corresponding histogram.

APPENDIX

Table 3. The function policevs.m generates symbolically the n^{th} Chebyshev polynomial defined on domain $[0, r_{wall}]$.

```
function Tc1 = policevs(N1,rmax1)
syms x N rmax
Tc1=((2.*x./rmax-1+sqrt((2.*x./rmax-1).^2-1)).^(N-1) +...
 (2.*x./rmax-1-sqrt((2.*x./rmax-1).^2-1)).^(N-1))./2;
 Tc2=subs(Tc1,N,N1);        %replace N by N1
 Tc1=subs(Tc2,rmax,rmax1);   %replace rmax by rmax1
```

Examples:

```
>> policevs(1,3)
        ans = 1
>> policevs(2,3)
        ans = 2/3*x-1
>> policevs(3,3)
        ans = 1/2*(2/3*x-1+((2/3*x-1)^2-1)^(1/2))^2+1/2*(2/3*x-1-((2/3*x-1)^2-1)^(1/2))^2
>> policevs(4,3)
        ans = 1/2*(2/3*x-1+((2/3*x-1)^2-1)^(1/2))^3+1/2*(2/3*x-1-((2/3*x-1)^2-1)^(1/2))^3
>> policevs(5,3)
        ans = 1/2*(2/3*x-1+((2/3*x-1)^2-1)^(1/2))^4+1/2*(2/3*x-1-((2/3*x-1)^2-1)^(1/2))^4
```

Table 4. Functions to generate symbolically the integrands

Integrals: $U(r)\cdot T_n^*(r)\cdot T_m^*(r)\cdot w(r)$

```
function Tmn=produsJ(M1,N1,rmax,q)
 syms x
   Tx=policevs(N1,rmax);Ty=policevs(M1,rmax);
   W=1./sqrt(1-(2.*x./rmax-1).^2);
   U=a+exp(-(x.^2)) ;
   Tmn=U.*Tx.*Ty.*W;
```

Integrals: $r^{-1}W(r)\cdot T_n^*(r)\cdot T_m^*(r)\cdot w(r)$

```
function Tmn=produsK(M1,N1,rmax,q)
 syms x
   Tx=policevs(N1,rmax);Ty=policevs(M1,rmax);
   W=1./sqrt(1-(2.*x./rmax-1).^2);
   Wsupr=q.*(1-exp(-(x.^2)))./(x.^2);
   Tmn=Wsupr.*Tx.*Ty.*W;
```

Integrals: $r\cdot U(r)\cdot T_n^*(r)\cdot T_m^*(r)\cdot w(r)$

```
function Tmn=produsL(M1,N1,rmax,q)
 syms x
   Tx=policevs(N1,rmax);Ty=policevs(M1,rmax);
   W=1./sqrt(1-(2.*x./rmax-1).^2);
   rU=x.*(a+exp(-(x.^2)));
   Tmn=rU.*Tx.*Ty.*W;
```

Integrand: $W(r)\cdot T_n^*(r)\cdot T_m^*(r)\cdot w(r)$

```
function Tmn=produsM(M1,N1,rmax,q)
 syms x
   Tx=policevs(N1,rmax);Ty=policevs(M1,rmax);
   W=1./sqrt(1-(2.*x./rmax-1).^2);
   Ww=q.*(1-exp(-(x.^2)))./x;
   Tmn=Ww.*Tx.*Ty.*W;
```

Integrals: $r \cdot W'(r) \cdot T_n^*(r) \cdot T_m^*(r) \cdot w(r)$

```
function Tmn=produsO(M1,N1,rmax,q)
 syms x
   Tx=policevs(N1,rmax);Ty=policevs(M1,rmax);
   W=1./sqrt(1-(2.*x./rmax-1).^2);rWder=x.*(q.*(  2.*exp(-(x.^2))+(  exp(-(x.^2))-1  )./(x.^2)
));
   Tmn=rWder.*Tx.*Ty.*W;
```

Integrals: $U'(r) \cdot T_n^*(r) \cdot T_m^*(r) \cdot w(r)$

```
function Tmn=produsP(M1,N1,rmax,q)
 syms x
   Tx=policevs(N1,rmax);Ty=policevs(M1,rmax);
   W=1./sqrt(1-(2.*x./rmax-1).^2);
   Uder=(-2.*x.*exp(-(x.^2)));
   Tmn=Uder.*Tx.*Ty.*W;
```

The integrals

$$I_{ij} = \int_0^{r_{wall}} rT_i^* T_j^* w\, dr \qquad J_{ij} = \int_0^{r_{wall}} UT_i^* T_j^* w\, dr \qquad K_{ij} = \int_0^{r_{wall}} \frac{W}{r} T_i^* T_j^* w\, dr$$

$$L_{ij} = \int_0^{r_{wall}} rUT_i^* T_j^* w\, dr \qquad M_{ij} = \int_0^{r_{wall}} WT_i^* T_j^* w\, dr \qquad O_{ij} = \int_0^{r_{wall}} rW'T_i^* T_j^* w\, dr$$

$$P_{ij} = \int_0^{r_{wall}} U'T_i^* T_j^* w\, dr$$

are numerically evaluated by means of function integrala.m, given in Table 4.

Table 4. Function integrala.m.

```
function valoareint = integrala(functie,lim1,lim2)
tt=sym2str(functie);
f=strcat('@(x)', tt);
fn=eval(f);
valoareint=quad(fn,lim1,lim2);
```

The results are retained in seven square $N \times N$ matrices. (see Table 5).

Table 5. Sequence for construction of the evaluation matrices.

```
I=zeros(N); J=zeros(N); K=zeros(N); L=zeros(N);
M=zeros(N); O=zeros(N); P=zeros(N);
for i=1:N
        for j=1:N
            I(i,j)=integrala(produsI(i,j,rmax),0,rmax);
            J(i,j)=integrala(produsJ(i,j,rmax,a),0,rmax);
            K(i,j)=integrala(produsK(i,j,rmax,q),0,rmax);
            L(i,j)=integrala(produsL(i,j,rmax,a),0,rmax);
            M(i,j)=integrala(produsM(i,j,rmax,q),0,rmax);
            O(i,j)=integrala(produsO(i,j,rmax,q),0,rmax);
            P(i,j)=integrala(produsP(i,j,rmax),0,rmax);
        end
end
```

CONCLUSIONS

This paper reports a numerical spectral approach based on shifted Chebyshev polynomials for numerically solving hydrodynamic eigenvalue problems with sophisticated boundary conditions. Numerical results showed that the use of this method improved the computational time and the obtained critical values of the eigenparameter involved are fairly accurate. The numerical results have been compared with other existing spatial investigations [3] and [9]. The collocation method proved to be more accurate, however the projection method was less expensive with respect to the numerical implementation costs, i.e. numerical results were obtained for a much smaller number of terms in the discretization. The results are very useful not only from their numerical values point of view, but also for their physical interpretation in fluid dynamics in flow control problems.

REFERENCES

[1.] Alekseenko, S.V., Kuibin, P.A., Okulov, V.L., Theory of concentrated vortices, Springer-Verlag Berlin Heidelberg, 2007.

[2.] Batchelor, G.K, Gill, A.E., Analysis of the stability of axisymmetric jets, J. Fluid Mech.,Vol. 14, 529 -551, 1962.
[3.] Bistrian, D.A., Dragomirescu, I., Savii, G., Descriptor Techniques for Modeling of Swirling Fluid Structures and Stability Analysis, WSEAS Transactions On Mathematics, Issue 1, Volume 9, pp. 56-66, ISSN: 1109-2769, 2010.
[4.] Bourne, D., Hydrodynamic stability, the Chebyshev tau method and spurious eigenvalues, Continuum Mech. Thermodyn. 15. Springer-Verlag, 571-579, 2003.
[5.] Canuto, C. et al., Spectral methods - Evolution to complex geometries and applications to fluid dynamics, Springer New York, 2007.
[6.] Dongara, J., Straughan, B.,Walker, D.W., Chebyshev tau - QZ algorithm, methods for calculating spectra of hydrodynamic stability problems, University of Tennessee, Computer Science Technical Report. UT-CS-95-294, 1995.
[7.] Gardner, D.R., Trogdon, S.A., Douglas, R.W.: A modified tau spectral method that eliminates spurious eigenvalues, J. Comput. Phys. 80, 137-167, 1989.
[8.] McFadden, G.B., Murray, B.T., Boisvert, R.F., Elimination of spurious eigenvalues in the Chebyshev tau spectral method, J. Comput. Phys. 91, 228-239, 1990.
[9.] Olendraru, C., Sellier, A., Rossi, M., Huerre, P., Inviscid instability of the Batchelor vortex: Absolute-convective transition and spatial branches, Physics of Fluids 11, 1805-1820, 1999.
[10.] Pozrikidis, C., Fluid dynamics, Theory, Computation and Numerical Simulation, Kluwer Academic Publishers, Boston, 2001.
[11.] Straughan, B., Porous convection, the Chebyshev tau method, and spurious eigenvalues, In: Straughan, B., Greve, R., Ehrentraut, H., Wang,Y. (eds.): Continuum Mechanics and Applications in Geophysics and the Environment, Berlin, Heidelberg, NewYork, Springer, 140-152, 2001.
[12.] Susan-Resiga, R., Ciocan, G.D., Anton, I., Avellan F., Analysis of the swirling flow downstream a francis turbine runner, Journal of Fluids Engineering 128, 177-189, 2006.
[13.] Tadmor, E., The exponential accuracy of Fourier and Chebyshev di®erencing methods, Siam Journal on Numerical Analysis, Vol.23, No.1, 1-10, 1986.
[14.] Trefethen, L.N., Spectral methods in Matlab, SIAM Philadelphia, 2000.
[15.] www.mathworks.com/matlabcentral/fileexchange/authors/30690
[16.] www.mathworks.com/help/techdoc/ref/strcat.html
[17.] www.mathworks.com/help/techdoc/ref/eval.html
[18.] www.mathworks.com/help/techdoc/ref/quad.html
[19.] www.mathworks.com/help/toolbox/pde/ug/sptarn.html

ANNALS OF FACULTY ENGINEERING HUNEDOARA
– INTERNATIONAL JOURNAL OF ENGINEERING